Results in Physics 8 (2018) 316–323

Contents lists available at ScienceDirect

Results in Physics

journal homepage: www.journals.elsevier.com/results-in-physics

Thermophysical analysis for three-dimensional MHD stagnation-point flow of nano-material influenced by an exponential stretching surface

Fiaz Ur Rehman [a,*], Sohail Nadeem [b], Hafeez Ur Rehman [c], Rizwan Ul Haq [d]

[a] Department of Mathematics, Govt. Postgraduate College No. 1, Abbottabad 22010, Pakistan
[b] Department of Mathematics, Quaid-I-Azam University, Islamabad 44000, Pakistan
[c] Department of Computer Science, National University of Computer and Emerging Sciences, Peshawar, Pakistan
[d] Department of Electrical Engineering, Bahria University, Islamabad Campus, Islamabad 44000, Pakistan

ARTICLE INFO

Article history:
Received 12 October 2017
Received in revised form 10 December 2017
Accepted 11 December 2017
Available online 16 December 2017

Keywords:
Heat transfer
Nanofluids
Stagnation-point flow
Three-dimensional flow
Nano particles
Boundary layer

ABSTRACT

In the present paper a theoretical investigation is performed to analyze heat and mass transport enhancement of water-based nanofluid for three dimensional (3D) MHD stagnation-point flow caused by an exponentially stretched surface. Water is considered as a base fluid. There are three (3) types of nanoparticles considered in this study namely, CuO (Copper oxide), Fe_3O_4 (Magnetite), and Al_2O_3 (Alumina) are considered along with water. In this problem we invoked the boundary layer phenomena and suitable similarity transformation, as a result our three dimensional non-linear equations of describing current problem are transmuted into nonlinear and non-homogeneous differential equations involving ordinary derivatives. We solved the final equations by applying homotopy analysis technique. Influential outcomes of aggressing parameters involved in this study, effecting profiles of temperature field and velocity are explained in detail. Graphical results of involved parameters appearing in considered nanofluid are presented separately. It is worth mentioning that Skin-friction along x and y-direction is maximum for Copper oxide-water nanofluid and minimum for Alumina-water nanofluid. Result for local Nusselt number is maximum for Copper oxide-water nanofluid and is minimum for magnetite-water nanofluid.

Introduction

The in depth study of flow phenomena focusing on stagnation-point flows and stretching surface is vital in the field of fluid mechanics and it has gained concentration of researchers after its useful practical applications in the industry, like flows observed over the tip of aircrafts and submarines. The spinning, floating and blowing of fiber glass is one of the best examples where flow caused by stretching plate near stagnation point can be detected. Hiemenz [1] was the leading researcher who investigated steady 2-D stagnation point flow and found its exact solution. Similarly, Howath [2] studied the flow near time-independent axisymmetric stagnation point. After that many researchers are involved in the study of flows involving stagnation point phenomena, like Chiam [3], Mahapatra and Gupta [4,5], Nazar et al. [6], Reza and Gupta [7], Lok et al. [8,9], etc. The researchers investigated the problem of boundary layers flow with heat transport effects when a sheet is stretched. Chiam [3] reported the 2-D stagnation-point flow in combination with stretching sheet problem and he revealed the interesting outcome that flow profile closer to stretching surface shows similar behavior as inviscid flow which is far away from surface yielding a nowhere boundary layer flow. Mahapatra and Gupta [5] illustrated contrary to the outcomes of Chiam [3]. There are a notable number of papers in the literature in which flow describing stagnation-point phenomena owing to a stretching sheet/surface is center of the study. Some of them include Ul Haq et al. [10], Rosali et al. [11], Mabood et al. [12], Hsiao [13] and Ur Rehman et al. [14], among others.

Enhancement of heat transfer by using nanofluids have attracted a lot of researcher because of their applications in fields like biocatalysis, bio-labeling, biosensors, purification and separation of biomolecules, transportation (Cooling of engine/thermal management of vehicle), cooling in nuclear systems, thermal storage, solar water heating, material manufactured by aerodynamic excursion and polymer excursion, glass fiber production, space, defense, magnetic resonance imaging (MRI), drug delivery, thermal absorption system etc. Choi [15] was the first researcher who used the word "nanofluids" at the ASME Winter Annual Meeting in 1995. From the appraisal of thermal assets it is a major problem with conventional heat transport liquids like bio-fluids, ethylene glycol, water, oil and lubricants that they lack in greater heat trans-

---

* Corresponding author.
E-mail address: tanolig@gmail.com (F. Ur Rehman).

https://doi.org/10.1016/j.rinp.2017.12.026
2211-3797/© 2017 The Authors. Published by Elsevier B.V.

Nomenclature

C_p	Specific heat, (Jkg^{-1} K$^{-1)}$
ρC_p	Heat capacitance
Nu	Nusselt number
L	Reference length
k	Thermal conductivity
p	Dimensional pressure
Pr	Prandtl number
A	Temperature exponent
T_∞	Ambient fluid temperature
T	Temperature
u	Component of velocity along x-axis
v	Components of velocity along y-axis
x	Cartesian co-ordinate along x-axis
y	Cartesian co-ordinate along y-axis
U	Dimensionless velocity along x-axis
V	Dimensionless velocity along y-axis
X	Dimensionless Cartesian component along x-axis
Y	Dimensionless Cartesian component along y-axis
U_s	Free stream velocity along x-axis
V_s	Free stream velocity along y-axis
c_{fx}	Skin friction coefficient along x-axis
c_{fy}	Skin friction coefficient along y-axis

α_1	Stretching ratio along x-axis
α_2	Stretching ratio along y-axis
Re	Reynolds number
M	Hartmann number
r_1	Stagnation point parameter

Greek Symbols

ρ	Fluid density
α	Thermal diffusivity
υ	Kinematic viscosity
ϕ	Volume fraction
η	Similarity variable
σ^*	Electrical conductivity
μ	Dynamic viscosity

Subscripts

f	Fluid
s	Particle
nf	Nanofluid
w	Wall conditions

fer characteristics. In fact, one solution to enhance thermal conductivity is to introduce nanoparticles in base fluids. Nanofluids are interesting to investigate because of their property to exhibit greater heat transfer characteristics as compared to other conventionally used heat transport fluids. An advanced method of amending thermal conductivity of common fluids is to introduce small size (1–100 nm) solid particles (nanoparticles) in fluid (base fluid). Lower thermal conductivity of common fluids impedes high concentration and effectivity of heat exchanger devices. The thermal conductivity possessed by new fluid which includes suspended nanoparticles is anticipated to be more eminent than common fluids. Many researchers have worked on the problems dealing nanofluids, both theoretically and experimentally. While making different nanoparticles, researchers used different materials to create them. Some of them include oxide ceramics (Al_2O_3, CuO), metals (Cu, Au, Ag), Ferro particles ($Fe_3O_4, CoFe_2O_4, Mn-ZnFe_2O_4$), metal nitrides ($SiN, AlN$), carbon in various (carbon nanotubes, diamond, graphite) and functional nanoparticles. Maxwell [16] was the first who introduced classical model. A list of review papers on nanofluids can be found in Refs. [17–19]. Bhattacharyya et al. [20] explored the heat transport caused by the stagnation-point flow when the sheet was shrunk exponentially. Bachok et al. [21] investigated the 3D stagnation flow in a nanofluid. The heat and mass transport problem of nanofluids over an exponentially stretched surface was investigated by Nadeem and Lee [22]. Nadeem et al. [23] reported results for heat transfer investigation for water-based nanofluid over an exponentially stretched surface and considered three different nanoparticles which include copper, alumina and titania. Vajravelu et al. [24] studied thermal radiation effects on nanofluids flow at a stagnation point over a stretching/shrinking surface with porous medium. Hsiao [25] studied mix convection and radiation impact on nanofluid flow with multimedia physical features. Noghrehabadi et al. [26] investigated flow and heat transport of nanofluids near the extrusion slit over a stretching sheet. Nadeem et al. [27] reported heat transfer analysis of Williamson nanofluid. Hsiao [28] investigated heat transport due to sinusoidal wall temperature of elastic-viscous fluid with unsteady oblique stagnation point flow due to over an oscillating-stretching surface. Some current work related to nanofluids can be reviewed from [29–47].

After reviewing available work, motivation of the present study is to investigate heat transport enhancement for MHD three-dimensional stagnation point fluid flow for water-based nanofluids. In this communication, water is treated as base fluid and effects of nanoparticle volume fraction are also taken into the account. We have taken three (3) kinds of nanoparticles with different thermophysical properties. They are CuO (Copper oxide), Fe_3O_4 (Magnetite), and Al_2O_3 (Alumia). It is worth mentioning that in this paper we considered nanofluid model projected by Tiwari and Das [48], which was also considered by several researchers [49–51]. Further, we employed an appropriate self-similar transformation to cut down modeled equations after invoking boundary-layer assumptions, to a group of nonlinear ODEs. Finally the leading equations are tackled by using HAM. To make sure convergence of desired solution, we plotted h-curve and constructed a convergence table. With the help of plotted graphs, we observed the impact of all parameters involved in this study. At last, tables are displayed to elaborate the outcomes of significant parameters against coefficient of skin friction & Nusselt number.

Mathematical analysis of the problem

We now consider a time-independent, laminar, 3-Dimensional MHD stagnation-point flow with water-based nanoparticles caused by an exponentially stretching surface, having velocity components U_w and V_w in two directions of Cartesian coordinate system (x, y, z) moving through a quiescent incompressible viscous fluid (see Fig. 1). The surface is settled at $z = 0$ and flow is bound to $z \geq 0$. The fluid observes continuous effect of a constant magnetic field expressed as $\boldsymbol{B}_0$ which is enforced in the z-direction orthogonal to xy-plane. Due to this influence, fluid under consideration is electrically conducted. It is important to note that induced magnetic field is missing because of the fact that magnetic Reynolds number is very small. Moreover, T_w and T_∞ are constant temperature experienced at wall and ambient fluid temperature respec-

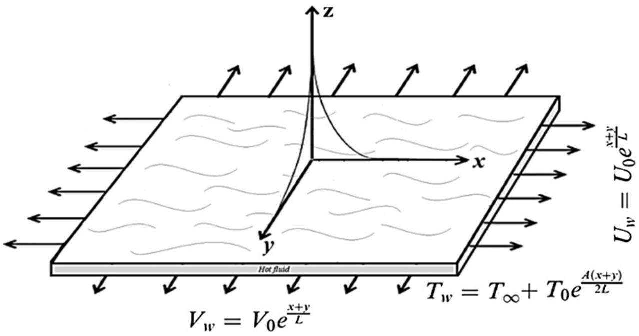

Fig. 1. Geometrical configuration of flow problem.

tively. After applying above suppositions the governing equation [34] can be represented in usual notations as:

$$u_x + v_y + w_z = 0, \tag{1}$$

$$uu_x + vu_y + wu_z = -\frac{1}{\rho_{nf}} p_x + \nu_{nf}\left(u_{zz} - \frac{\sigma^* B_0^2}{\rho} u\right), \tag{2}$$

$$uv_x + vv_y + wv_z = -\frac{1}{\rho_{nf}} p_y + \nu_{nf}\left(v_{zz} - \frac{\sigma^* B_0^2}{\rho} v\right), \tag{3}$$

$$uT_x + vT_y + wT_z = \alpha_{nf} T_{zz}, \tag{4}$$

Associated boundary conditions are

$$z = 0, u = U_w, v = V_w, w = 0, T = T_w, \tag{5}$$

$$z \to \infty, u = U_s(x,y), v = V_s(x,y), w = 0, T = T_\infty. \tag{6}$$

Here subscript 'w' refers the condition on wall. In this study we assumed that the surface stretching velocities, wall temperature and free stream velocity are

$$U_w(x,y) = U_0 e^{\frac{(x+y)}{L}}, V_w(x,y) = V_0 e^{\frac{(x+y)}{L}}, T_w(x,y) = T_\infty + T_0 e^{\frac{A(x+y)}{2L}}, \tag{7}$$

$$U_s(x,y) = U_e e^{\frac{(x+y)}{L}}, V_s(x,y) = V_e e^{\frac{(x+y)}{L}}, \tag{8}$$

where T_0, U_0, V_0, U_e and V_e are all constants, U_s and V_s are free stream velocities, T_∞ is ambient fluid temperature, L specifies reference length, and A intends the temperature exponent. The effective density ρ_{nf} and the effective viscosity μ_{nf} given by Brinkman [52], are expressed as

$$\mu_{nf} = \frac{\mu_f}{(1-\phi)^{2.5}}, \quad \rho_{nf} = \phi\rho_s + (1-\phi)\rho_f, \tag{9}$$

The heat capacitance $(\rho C_p)_{nf}$ and thermal diffusivity α_{nf} of nanofluid as given by Xuan and Li [53] are defined as

$$(\rho C_p)_{nf} = \phi(\rho c_p)_s + (\rho c_p)_f(1-\phi), \alpha_{nf} = \frac{k_{nf}}{(\rho C_p)_{nf}}, \tag{10}$$

The effective thermal conductivity k_{nf} and viscosity ν_{nf} are obtained experimentally [54] and are given by

$$\frac{k_{nf}}{k_f} = \frac{(k_s + 2k_f) - 2\phi(k_f - k_s)}{(k_s + 2k_f) + \phi(k_f - k_s)}, \quad \nu_{nf} = \frac{\mu_{nf}}{\rho_{nf}}, \tag{11}$$

A similarity transformation [23] is introduced as

$$u = U_e e^{\frac{(x+y)}{L}} f'(\eta), v = U_e e^{\frac{(x+y)}{L}} g'(\eta), w = -\left(\frac{\nu U_e}{2L}\right)^{1/2} e^{\frac{(x+y)}{2L}} [f + \eta f' + g + \eta g'],$$
$$T = T_\infty + T_0 e^{\frac{A(x+y)}{2L}} \theta(\eta), \eta = \left(\frac{U_e}{2\nu L}\right)^{1/2} e^{\frac{(x+y)}{2L}} z, \tag{12}$$

and our basic Eqs. (2)–(4) are transmuted into following three ordinary differential equations (ODEs):

$$\frac{1}{(1-\phi+\phi(\rho_s/\rho_f))(1-\phi)^{2.5}} f''' = -f''(f+g) + 2f'(f'+g') + M(f'-1) - 2(1+r_1), \tag{13}$$

$$\frac{1}{(1-\phi+\phi(\rho_s/\rho_f))(1-\phi)^{2.5}} g''' = -g''(f+g) + 2g'(f'+g') + Mr_1(g'-1) - 2(1+r_1)r_1, \tag{14}$$

$$\frac{1}{\mathbf{Pr}}\left[\frac{k_{nf}/k_f}{(1-\phi) + \phi\left((\rho c_p)_s/(\rho c_p)_f\right)}\right]\theta'' = -(f+g)\theta' + A(f'+g')\theta, \tag{15}$$

Now corresponding boundary conditions (5) and (6) become

$$f(0) = 0 = g(0), f'(0) = \alpha_1, g'(0) = \alpha_2, \theta(0) = 1, \tag{16}$$

$$f'(\infty) = 1, g'(\infty) = r_1, \theta(\infty) = 0. \tag{17}$$

Here the primes stand for differentiation of function with respect to η, $\alpha_1 = U_0/U_e$ and $\alpha_2 = V_0/U_e$ represent wall stretching ratios, $r_1 = V_e/U_e$ is stagnation point, $M = \frac{\sigma B_0^2}{\rho U_s}$ is the Hartmann number and $Pr = (\mu c_p)_f/k_f$ is referred as the Prandtl number. The first two terms in Eq. (16) arise from the no-penetration wall condition, $f(0) + g(0) = 0$. Without loss of generality, Eq. (16) is used instead. Note that the continuity Eq. (1) has been satisfied by assuming the form defined in Eq. (12). Eqs. (13)–(17) demonstrate that the non-homogeneous hydrodynamic problem contains three parameters in the boundary conditions, on the other hand heat transport problem contains two additional parameters in the equation.

The physical properties of much importance are the dimensionless coefficients of surface skin-friction c_{fx} and c_{fy}, along both directions, and the local Nusselt number defined as

$$c_{fx} = \frac{\tau_{wx}}{\rho_f U_0^2/2}, \quad c_{fy} = \frac{\tau_{wy}}{\rho_f U_0^2/2}, \quad Nu_x = \frac{xq_w}{k_f(T - T_\infty)}, \tag{18}$$

where τ_{wx} and τ_{wy} are shear stresses in the x- and y-directions, respectively, and q_w represents heat flux of surface. These are defined as

$$\tau_{wx} = \mu_{nf}(u_z + w_x)_{z=0}, \tau_{wy} = \mu_{nf}(v_z + w_y)_{z=0}, q_w = -k_{nf} T_z|_{z=0}, \tag{19}$$

Using Eqs. (12) and (19), we get

$$Re_x^{1/2} C_{fx}/2e^{\frac{3(x+y)}{2L}} = \frac{1}{(1-\phi)^{2.5}} f''(0), \tag{20}$$

$$Re_y^{1/2} C_{fy}/2e^{\frac{3(x+y)}{2L}} = \frac{1}{(1-\phi)^{2.5}} g''(0), \tag{21}$$

$$Re_x^{-1/2} N_{u_x}/2e^{\frac{x+y}{2L}} \frac{x}{L} = -\frac{k_{nf}}{k_f}\theta'(0), \tag{22}$$

where Re symbolizes Reynolds number defined as $Re = U_0 L/\nu$.

Solution technique

To obtain the solutions of Eqs. (13)–(15), we adopted frequently used Homotopy analysis technique (HAM) [54–58]. It is a powerful analytic type technique for solving non-linear, ordinary as well as partial differential equations. In 1992, Liao developed this analytical technique. This technique can be used to solve weak as well as strongly non-linear mathematical models due to the fact that it does not dependent on small physical parameter confinement. While using this technique we can adapt the convergence of solution using base functions and supplementary parameters. In the present study our initial guesses and their corresponding operators are listed below

$$\left.\begin{aligned} f_0(\eta) &= \eta + (\alpha_1 - 1) * (1 - \exp(-\eta)), \\ g_0(\eta) &= (\alpha_2 - r_1) + r_1 * \eta + (r_1 - \alpha_2) * (1 - \exp(-\eta)), \\ \theta_0(\eta) &= exp(-2\eta). \end{aligned}\right\} \quad (23)$$

$$\mathcal{L}_f = \frac{d^3 f}{d\eta^3} - \frac{df}{d\eta}, \quad \mathcal{L}_g = \frac{d^3 g}{d\eta^3} - \frac{dg}{d\eta}, \quad \mathcal{L}_\theta = \frac{d^2\theta}{d\eta^2} - 4\theta, \quad (24)$$

Convergence analysis

The rapid convergence of generated solution after employing Homotopy analysis technique greatly relies on the best selection of supplementary parameter $\hbar_f, \hbar_g, \hbar_\theta$. The usefulness of obtained solution highly depends on the rate of convergence. Hence we have diagrammed $\hbar$-curves for *CuO*-water in Fig. 2 in order to obtain the legitimate values of $\hbar_f, \hbar_g$ and $\hbar_\theta$.

After going through Fig. 2 we observe that the permissible range for auxiliary parameters is $-1.3 \le \hbar_f, \hbar_g \le -0.3, -1.7 \le \hbar_\theta \le -0.2$. It is observed that the series solution will be convergent in the whole realm of $\eta (0 < \eta < \infty)$ by selecting $\hbar_f = \hbar_g = \hbar_\theta = -0.75$. After investigation of outcomes in above table, it is guaranteed that the desired convergence is attained at 30th order.

Final outcomes and discourse of results

In the present section we shall thoroughly explain the behavior of important parameters on dimensionless velocities, temperature, skin frictions and heat transport for (water-based) nanofluid. The egressing parameters are nanoparticle volume fraction ϕ, stretching parameters α_1 and α_2, stagnation point parameter r_1, Hertmann number M, and temperature exponent parameter A as shown in Figs. 3–16 for water-based nanofluids. There are three characters of nanoparticles under consideration in the present study namely, *CuO* (Copper oxide), Fe_3O_4 (Magnetite), and Al_2O_3 (Alumina). These three nanoparticles were also considered by different researcher [21,23,30,31,59] for different heat transport problems. In the investigation conducted by Oztop and Abu-Nada [59], they selected $\mathrm{Pr} = 6.2$ (for water) and ϕ is taken as $0 \le \phi \le 0.2$ where $\phi = 0$ refers the Newtonian type fluid. Also we have listed thermophysical characteristics of chosen base fluid (water) and three different nanoparticles (1–100 nm) in Table 2.

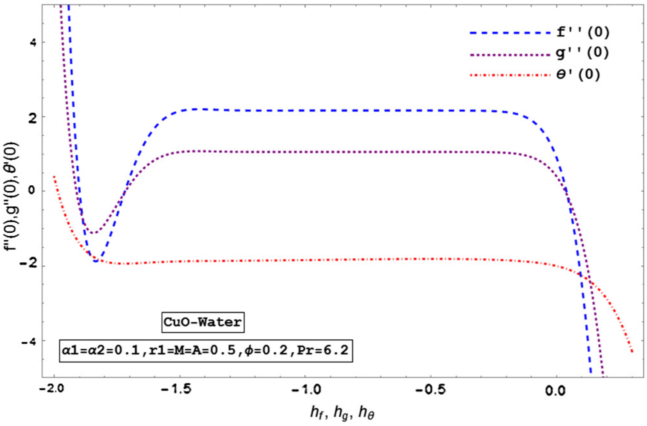

Fig. 2. $\hbar-$ curves for the functions $f(\eta), g(\eta)$ and $\theta(\eta)$.

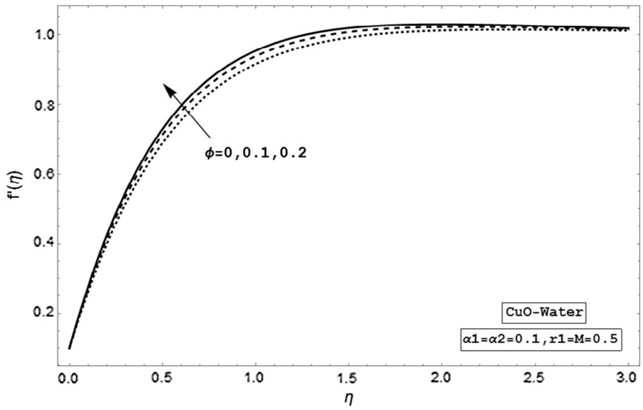

Fig. 3. Variation of ϕ influencing velocity profile $f'(\eta)$.

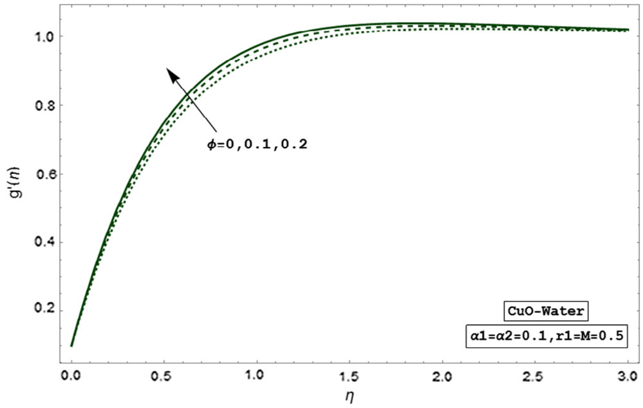

Fig. 4. Variation of ϕ influencing velocity profile $g'(\eta)$.

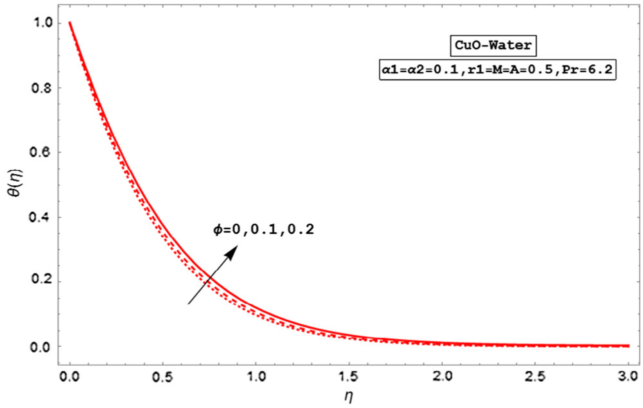

Fig. 5. Variation of ϕ influencing temperature profile $\theta(\eta)$.

From graphical results we observed that in presence of magnetic effects and stagnation point flow all velocities $f'(\eta)$ and $g'(\eta)$ start from their wall values $\alpha 1$ and $\alpha 2$ respectively. As η increases, $f'(\eta)$ approaches 1 and $g'(\eta)$ approaches the stagnation point r1. The temperature profile $\theta'(\eta)$ decreases from unity (1) to zero (0) as dimensionless distance η grows from starting position zero to infinity. This section contains Figs. 3–16. These Figures are exhibited in order to see the exciting results of several parameters which effect velocity and temperature behavior. Figs. 3–5

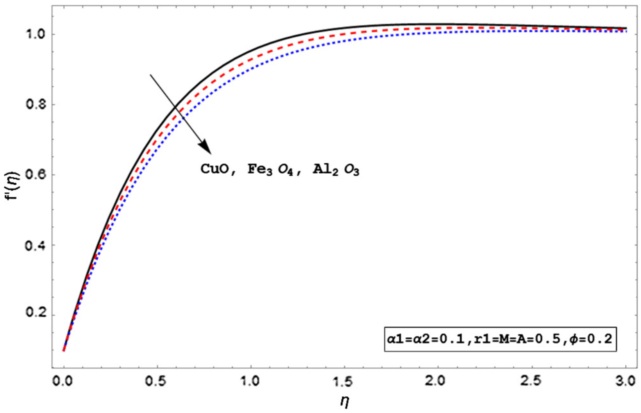

Fig. 6. Influence of nanoparticles on velocity profile $f'(\eta)$.

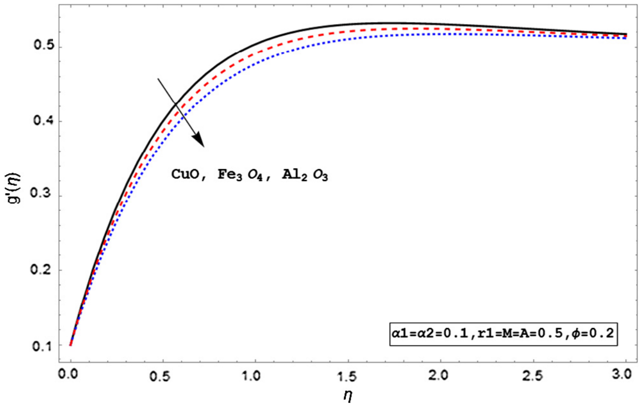

Fig. 7. Influence of nanoparticles on velocity profile $g'(\eta)$.

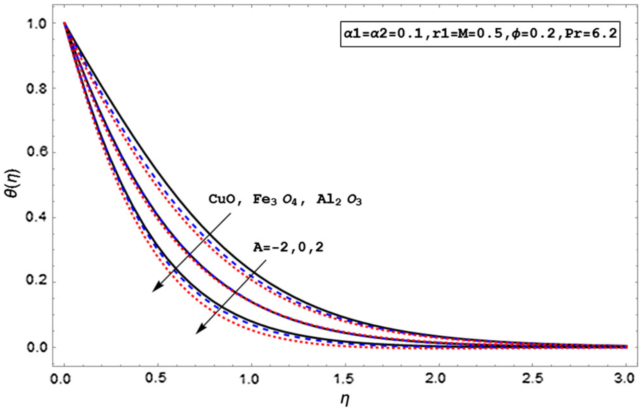

Fig. 8. Influence of nanoparticles on temperature profile $\theta(\eta)$.

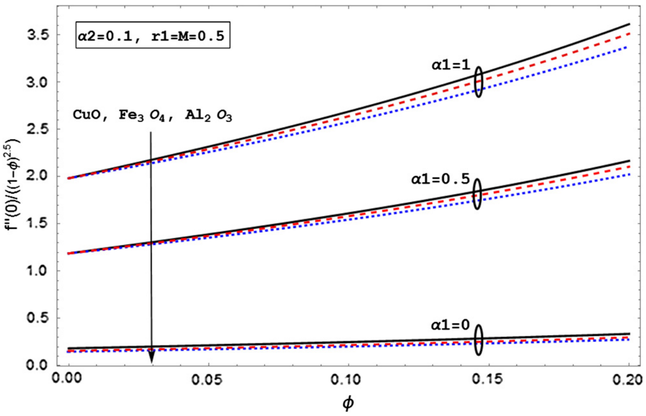

Fig. 9. Influence of ϕ and α_1 for different nanoparticles on skin friction coefficient along x-axis.

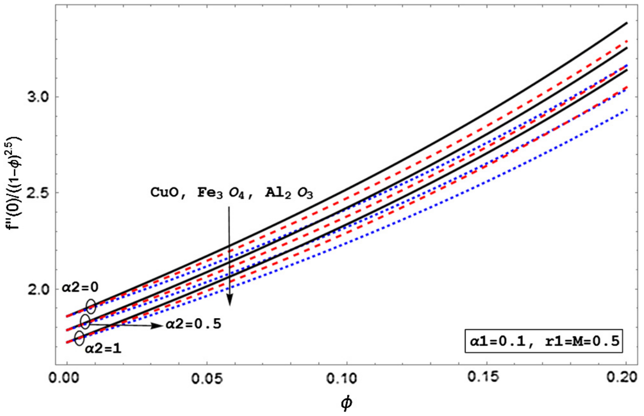

Fig. 10. Influence of ϕ and α_2 for different nanoparticles on skin friction coefficient along x-axis.

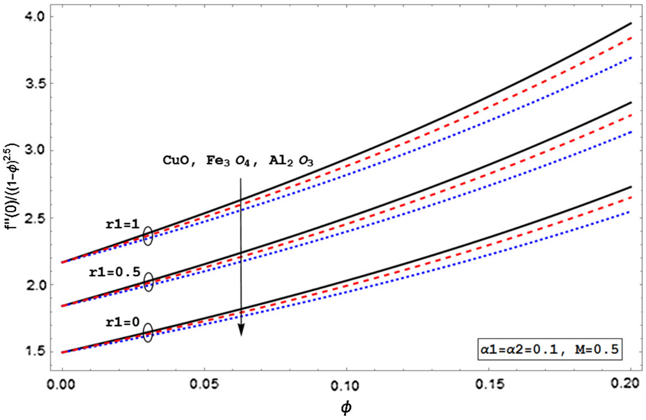

Fig. 11. Influence of ϕ and r_1 for different nanoparticles on skin friction coefficient along x-axis.

illustrates the consequences of CuO-nanoparticle volume fraction ϕ and stagnation point r_1 on the dimensionless velocity as well as temperature profiles. It is observed that an enhancement in ϕ tends to a growing behavior in the dimensionless velocities and temperature. As stagnation pointr$_1(\geq \alpha_2)$ increases, the dimensionless velocities show an increase whereas temperature profile tends to decrease.

Figs. 6–8 elucidate the influence of different nanoparticles under consideration including Copper oxide (CuO), Magnetite (Fe_3O_4), and alumina (Al_2O_3) and they are effecting velocity, temperature profiles. From Figs. 6 and 7 we can easily analyze that CuO–water nanofluid has maximum velocity in comparison with Fe_3O_4–water and Al_2O_3–water nanofluids in both directions.

It also explains the maximum velocity of Fe_3O_4–water nanofluid over Al_2O_3–water nanofluid. Fig. 8 explains the thermal boundary layer is thicker for Al_2O_3–water nanofluid as compared to the other two. Also by increasing the temperature exponent parameter A, we conclude enhancement in thickness of boundary layer (thermal) is noticed. In absence of magnetic field and taking $\alpha_2 = r_1 = 0$, we

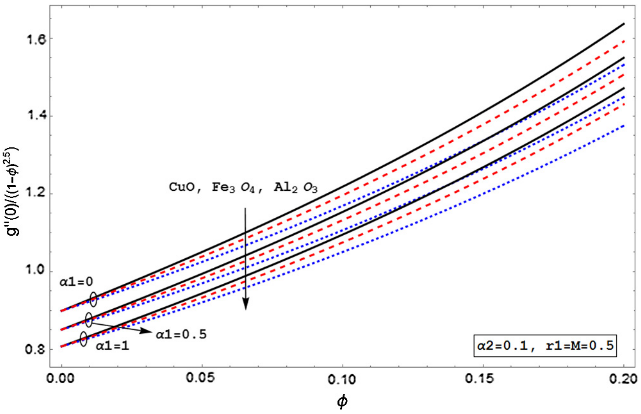

Fig. 12. Influence of ϕ and α_1 for different nanoparticles on skin friction coefficient along y-axis.

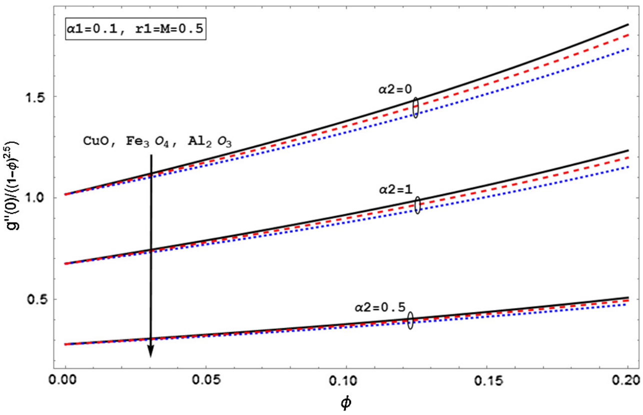

Fig. 13. Influence of ϕ and α_2 for different nanoparticles on skin friction coefficient along y-axis.

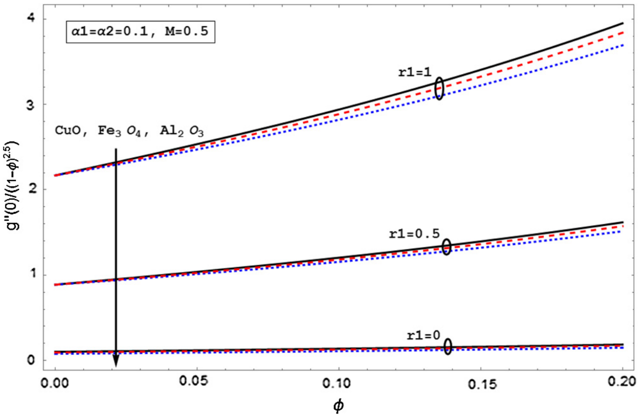

Fig. 14. Influence of ϕ and α_1 for different nanoparticles on skin friction coefficient along y-axis.

compared the current study (Al_2O_3–water nanofluid) with literature [44] in Table 3. Both results represented in Table 3 show a good agreement. Therefore we believe that present results are accurate.

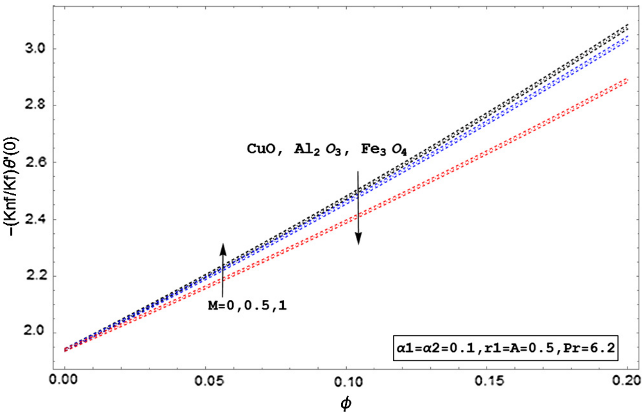

Fig. 15. Influence of ϕ and M for different nanoparticles on Nusselt number.

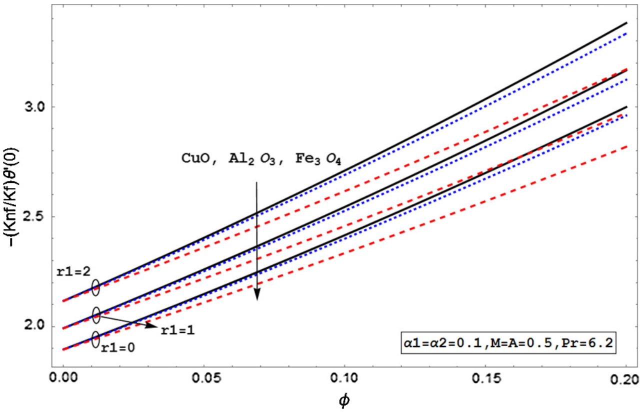

Fig. 16. Influence of ϕ and r_1 for different nanoparticles on Nusselt number.

Table 1
Convergence of Homotopy solution for ***CuO***-Water when $\boldsymbol{r_1} = 0.5, \alpha_1 = \alpha_2 = \phi = 0.1, \boldsymbol{Pr} = 6.2, \mathbf{A} = \mathbf{M} = 0.5, \hbar_f = \hbar_g = \hbar_\theta = -0.75$.

Order of approximation	$-f''(0)$	$-g''(0)$	$-\theta'(0)$
1	1.747	0.834	1.925
10	2.171	1.060	1.805
20	2.169	1.061	1.835
30	2.169	1.061	1.859
40	2.169	1.061	1.859
50	2.169	1.061	1.859

Figs. 9–14 present the change in skin-friction with governing parameters α_1, α_2 and r_1 along x and y-direction respectively. In Figs. 9–11 it is depicted that the resistance to the flow in$x$ increases for increasing α_1 and $r_1$and falls for rising α_2. It is important to note that in each particular case along x-axis, the skin friction remained maximum for Copper Oxide-water nanofluid whereas minimum for Alumina-water nanofluid. On the other hand Figs. 12–14 explains that skin friction in y-direction increases for growing values of stagnation-pointr_1, and shows a decrease for growing values of stretching parametersα_1. As α_2 varies, the skin friction in y-direction is maximum for $\alpha_2 = 0$ and minimum for $\alpha_2 = 0.5$. In Figs. 12–14 for each particular case along y-axis, the skin friction remained maximum for Copper Oxide-water nanofluid whereas it was minimum for Alumina-water nanofluid. The fluctuation of heat transport rate with the governing parameters is shown in Figs. 15–17. It is quite evident from Fig. 15 that as Hertmann number M increases, the heat transport rate also increases. Also for varying values of M, The maximum heat flux is reported for Copper oxide-water nanofluid and minimum for magnetite-water nanofluid. Similar behavior can be observed for heat flux against temperature exponent parameter A and stagnation point parameter r_1 in Figs. 16 and 17.

Table 2
Thermophysical properties of considered nanoparticles along water [30,31].

Physical Properties	Base-Fluid (water)	**CuO**	**Al_2O_3**	**Fe_3O_4**
$C_p(\mathbf{J/kgK})$	4179	531.8	765	670
$\boldsymbol{k}(\mathbf{W/mK})$	0.613	76.5	40	9.7
$\rho(\mathbf{kg/m^3})$	997.1	6320	3970	36

Table 3
Comparison with the literature for stagnation-point flow of $\boldsymbol{Al_2O_3}$-water nanofluid $\boldsymbol{r}_1 = \alpha_2 = \boldsymbol{M} = 0, \boldsymbol{Pr} = 6.2, \mathbf{A} = 1, \hbar_{\boldsymbol{f}} = \hbar_{\boldsymbol{g}} = \hbar_\theta = -0.75$.

α_1	ϕ	$\frac{1}{(1-\phi)^{2.5}}\boldsymbol{f}''(0)$		$-\frac{\boldsymbol{k_{nf}}}{\boldsymbol{k_f}}\theta'(0)$	
		Bachok et al. [36]	Present results	Bachok et al. [36]	Present results
0	0	1.6872	1.6872	1.7148	1.7148
	0.1	2.1929	2.19293	2.0230	2.02301
	0.2	2.8174	2.81750	2.3345	2.33440
0.5	0	0.9604	0.96040	2.4874	2.48741
	0.1	1.2483	1.24829	2.8478	2.84784
	0.2	1.6039	1.60399	3.2235	3.22355

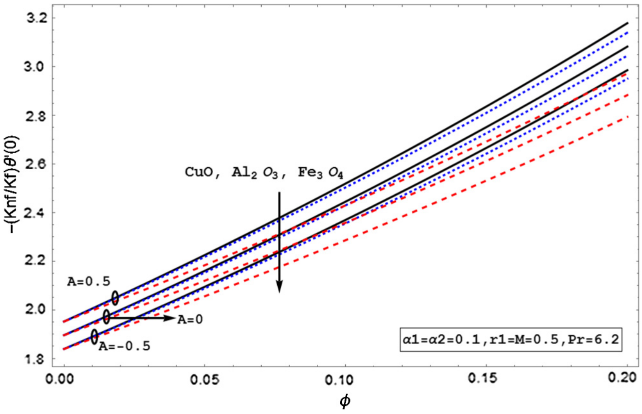

Fig. 17. Influence of ϕ and A for different nanoparticles on Nusselt number.

Concluding remarks

The whole investigation is reported for flow and heat transport enhancement for MHD 3-D stagnation-point flow of water-based nanofluid caused by a confined surface which is stretched exponentially. The suspended nanoparticles in current study were *CuO* (Copper oxide), Fe_3O_4 (Magnetite), and Al_2O_3 (Alumia). This study also assumes that the temperature specified at the surface varies exponentially. The developed mathematical model is tackled by homotopy analysis technique. We observed in current study that

- Nanoparticle volume fraction (symbolized as ϕ) appreciably enhances the dimensionless temperature and velocity field.
- Nanoparticle volume fraction also results in enhancement of skin friction and heat flux.
- The stagnation point parameter r_1 increases produced velocity and thermal profile whereas decreases induced boundary layer thickness in each case.
- Influence of temperature exponent (symbolized as **A**) is to increases temperature profile, thermal boundary layer and heat flux.
- From graphical results we can conclude that Skin-friction along *x* and *y*-direction is greater for *CuO*-water nanofluid and lesser for AL_2O_3–water nanofluid.
- The resulting quantity of local Nusselt number came out greater for *CuO*-water nanofluid whereas lesser for Fe_3O_4-water nanofluid.

Appendix A. Supplementary data

Supplementary data associated with this article can be found, in the online version, at https://doi.org/10.1016/j.rinp.2017.12.026.

References

[1] Hiemenz K. Die Grenzschicht an einem in den gleichformingen Flussigkeitsstrom eingetauchten graden Kreiszylinder. Dinglers Polytech J 1911;326:321–4.
[2] Howarth L. The boundary layer in three dimentionless flow-Part II, The flow near a stagnation point. Philos Mag (Series 7) 1951;42:1433–40.
[3] Chiam TC. Stagnation-point flow towards a stretching plate. J Phys Soc Japan 1994;63:2443–4.
[4] Mahapatra TR, Gupta AS. Magnetohydrodynamic stagnation point flow towards a stretching sheet. Acta Mech 2001;152:191–6.
[5] Mahapatra TR, Gupta AS. Heat transfer in stagnation point flow towards a stretching sheet. H. M. Trans 2002;38:517–21.
[6] Nazar R, Amin N, Filip D, Pop I. Stagnation-point flow of a micropolar fluid towards a stretching sheet. Int J Non-linear Mech 2004;39:1227–35.
[7] Reza M, Gupta AS. Steady two-dimensional oblique stagnation point flow towards a stretching surface. Fluid Dyn Res 2005;37:334–40.
[8] Lok YY, Amin N, Pop I. Non-orthogonal stagnation point flow towards a stretching sheet. Int J Non-linear Mech 2006;41:622–7.
[9] Lok YY, Pop I, Ingham DB, Amin N. Mixed convection flow of a micropoalr fluid near a non-orthogonal stagnation point on a stretching vertical sheet. Int J Numer Meth H Fluid Flow 2009;19:459–83.
[10] Haq RU, Nadeem S, Khan ZH, Akbar NS. Thermal radiation and slip effects on MHD stagnation point flow of nanofluid over a stretching sheet. Physica E 2015;65:17–23.
[11] Rosali H, Ishak A, Nazar R, Merkin JH, Pop I. The effect of unsteadiness on mixed convection boundary-layer stagnation point flow over a vertical flat surface embedded in a porous medium. Int J Heat Mass Transfer 2014;77:147–56.
[12] Mabood F, Khan WA, Md AI. Ismail, MHD stagnation point flow and heat transfer impinging on stretching sheet with chemical reaction and transpiration. Chem Eng J 2015;273:430–7.
[13] Hsiao K-L. Stagnation electrical MHD nanofluid mixed convection with slip boundary on a stretching sheet. Appl Ther Eng 2016;98:850–61.
[14] Rehman Fiaz Ur, Nadeem S, Haq RU. Heat transfer analysis for three-dimensional stagnation-point flow over an exponentially stretching surface. Chin J Phys 2017;55:1552–60.
[15] Chol SUS. Enhancing thermal conductivity of fluids with nanoparticles. Off Sci Tech Inf Tech Rep 1995;231(1):99–105.
[16] Hamilton RL, Crosser OK. Thermal conductivity of heterogeneous two component systems. I&EC Fund 1962;1:182–91.
[17] Pang C, Lee JW, Kang YT. Review on combined heat and mass transfer characteristics in nanofluids. Int J Therm Sci 2015;87:49–67.
[18] Sarkar J, Ghosh P, Adil A. A review on hybrid nanofluids: recent research, development and applications. Renew Sustain Energy Rev 2015;43:164–77.

[19] Bahiraei M, Hangi M. Flow and heat transfer characteristics of magnetic nanofluids: a review. J Magn Mater 2015;374:125–38.
[20] Bhattacharyya K, Vajravelu K. Stagnation-point flow and heat transfer over ab exponentially shrinking sheet. Commun Nonlinear Sci Numer Simulat 2012;17:2728–34.
[21] Bachok Anuar Ishak, Nazar Roslinda, Pop Ioan. Flow and heat transfer at a general three-dimensional stagnation point in a nanofluid. Physica B: Cond Matter 2010;405:4914–8.
[22] Nadeem S, Lee CH. Boundary layer flow of nanofluid over an exponentially stretching surface. Nanoscale Res. Lett. 2012;7. article 94.
[23] Nadeem S, Haq RU, Khan ZH. Heat transfer analysis of water-based nanofluid over an exponentially stretching sheet. Alexandria Eng J 2014;53(1):219–24.
[24] Pal D, Mandal G, Vajravelu K. Flow and heat transfer of nanofluids at a stagnation point flow over a stretching/shrinking surface in a porous medium with thermal radiation. Appl Math Comput 2014;238:208–24.
[25] Hsiao K-L. Nanofluid flow with multimedia physical features for conjugate mixed convection and radiation. Comput Fluid 2014;104:1–8.
[26] Noghrehabadi A, Izadpanahi E, Ghalambaz M. Analyze of fluid flow and heat transfer of nanofluids over a stretching sheet near the extrusion slit. Comput Fluid 2014;100:227–36.
[27] Nadeem S, Hussain ST. Flow and heat transfer analysis of Williamson nanofluid. Appl Nanosci 2014;4(8):1005–12.
[28] Hsiao K-L. Heat transport analysis of unsteady oblique stagnation point flow of elastic-viscous fluid due to sinusoidal wall temperature over an oscillating-stretching surface: A numerical approach. J Mol Liq 2016;219:748–55.
[29] Hsiao K-L. Stagnation Electrical MHD nanofluid mixed convection with slip boundary on a stretching sheet. Appl T.H. Eng 2016;98. 850-816.
[30] Haq RU, Noor NFM, Khan ZH. Numerical simulation of water based magnetite nanoparticles between two parallel disks. Adv Powder Tech 2016;27(4):1568–75.
[31] Hayat T, Nawaz S, Alsaedi A, Rafiq M. Mixed convective peristaltic flow of water based nanofluids with joule heating and convective boundary conditions. PLoS One 2016;11(4):e0153537.
[32] Khan M, Irfan M, Khan WA, Alshomrani AS. A new modeling for 3D Carreau fluid flow considering nonlinear thermal radiation. Results Phys 2017;7:2692–704.
[33] Hayat T, Khan MI, Waqas M, Alsaedi A, Farooq M. Numerical simulation for melting heat transfer and radiation effects in stagnation point flow of carbon-water nanofluid. Comp Methods Appl Mech Eng 2017;315:1011–24.
[34] Rehman Fiaz Ur, Nadeem Sohail. Heat transfer analysis for three-dimensional stagnation-point flow of water-based nanofluid over an exponentially stretching surface. ASME J Heat Transfer 2017. https://doi.org/10.1115/1.4038359.
[35] Irfan M, Khan M, Khan WA. Numerical analysis of unsteady 3D flow of Carreau nanofluid with variable thermal conductivity and heat source/sink. Results Phys 2017;7:3315–24.
[36] Khan M, Irfan M, Khan WA. Impact of forced convective radiative heat and mass transfer mechanisms on 3D Carreau nanofluid: A numerical study. Euro Phys J Plus 2017. https://doi.org/10.1140/epjp/i2017-11803-3.
[37] Khan WA, Irfan M, Khan M, Alshomrani AS, Alzahrani AK, Alghamdi MS. Impact of chemical processes on magneto nanoparticle for the generalized Burgers fluid. J Mol Liq 2017;234:201–8.
[38] Khan M, Irfan M, Khan WA. Impact of nonlinear thermal radiation and gyrotactic microorganisms on the Magneto-Burgers nanofluid. Int J Mech Sci 2017;130:375–82.
[39] Khan M, Irfan M, Khan WA, Ahmad L. Modeling and simulation for 3D magneto Eyring-Powell nanomaterial subject to nonlinear thermal radiation and convective heating. Results Phys 2017;7:1899–906.
[40] Khan WA, Irfan M, Khan M. An improved heat conduction and mass diffusion models for rotating flow of an Oldroyd-B fluid. Results Phys 2017;7:3583–9.
[41] Khan WA, Khan M, Irfan M, Alshomrani AS. Impact of melting heat transfer and nonlinear radiative heat flux mechanisms for the generalized Burgers fluids. Results Phys 2017;7:4025–32.
[42] Khan M, Irfan M, Khan WA. Numerical assessment of solar energy aspects on 3D magneto-Carreau nanofluid: A revised proposed relation. Int J Hydrogen Energy 2017;42:22054–65.
[43] Sheikholeslami Mohsen, Rokni Houman B. Effect of melting heat transfer on nanofluid flow in the presence of a magnetic field using the Buongiorno Model. Chin J Phys 2017;55(4):1115–26.
[44] Bachok Anuar Ishak, Pop Ioan. Boundary layer stagnation-point flow and heat transfer over an exponentially stretching/shrinking sheet in a nanofluid. Int J Heat Mass Transfer 2012;55:8122–8.
[45] Sheikholeslami M, Rokni HB. Influence of melting surface on MHD nanofluid flow by means of two phase model. Chin J Phys 2017;55(4):1352–60.
[46] Haq RU, Rashid Irfan, Khan ZH. Effects of aligned magnetic field and CNTs in two different base fluids over a moving slip surface. J Mol Liq 2017. https://doi.org/10.1016/j.molliq.2017.08.084.
[47] Hayat T, Nadeem S. Heat transfer enhancement with Ag-CuO/water hybrid nanofluid. Results Phys 2017;7:2317–24.
[48] Tiwari RK, Das MK. Heat transfer augmentation in a two-sided lid-driven differentially heated square cavity utilizing nanofluids. Int J Heat Mass Transfer 2007;50:2002–18.
[49] Abu-Nada E. Application of nanofluids for heat transfer enhancement of separated flows encountered in a backward facing step. Int J Heat Fluid Flow 2008;29:242.
[50] Abu-Nada E, Oztop HF. Effects of inclination angle on natural convection in enclosures filled with Cu-water nanofluid. Int J Heat Fluid Flow 2009;30:669–78.
[51] Talebi F, Houshang A, Shahi M. Numerical study of mixed convection flows in a square lid-driven cavity utilizing nanofluid. Int Commun Heat Mass Transfer 2010;37(1):79–90.
[52] Brikman HC. The viscosity of concentrated suspensions and solutions. J Chem Phys 1952;20:571–81.
[53] Xuan Y, Li Q. Investigation on convective heat transfer and flow features of nanofluids. ASME J Heat Transfer 2003;125:151–5.
[54] Li, Q., and Xuan, Y., 2000, "Experimental Investigation on Transport Properties of Nanofluids", Heat Transfer Science and Technology 2000, Wang Buxuan, ed., Higher Edu. Press., 757–762.
[55] Liao SJ. An approximate solution technique not depending on small parameters: a special example. Int J Non-linear Mech 1995;30(3):371–80.
[56] Liao SJ. Homotopy analysis method: a new analytic method for nonlinear problems. Appl Math Mech 1998;19(10):957–62.
[57] Liu CS. The essence of the homotopy analysis method. Appl Comp 2010;216:1299–303.
[58] Liao SJ. Beyond perturbation: introduction to the homotopy analysis method. CRC Press LLC; 2004.
[59] Oztop HF, Abu-Nada E. Numerical study of natural convection in partially heated rectangular enclosures filled with nanofluids. Int J Heat Fluid Flow 2008;29:1326–36.